Int. J. Heat Mass Transfer. Vol. 14, pp. 1771–1783. Pergamon Press 1971. Printed in Great Britain.

PREDICTION OF DEPARTURE DIAMETER AND BUBBLE FREQUENCY IN NUCLEATE BOILING IN UNIFORMLY SUPERHEATED LIQUIDS

M. SADDY† and G. J. JAMESON

Department of Chemical Engineering and Chemical Technology, Imperial College, London, S.W.7, England

(*Received* 4 *June* 1970 *and in revised form* 14 *October* 1970)

Abstract—A theory is presented to describe the motion of vapour bubbles growing at a nucleation site in a uniformly superheated liquid. By incorporating the classical theory for spherical phase growth, the equations of *translatory* motion were solved, enabling the radius and position of the bubble to be calculated as a function of time.

The theoretical results are compared with experiments using boiling water and acetic acid. For water the bubble radius was found to vary as (time)$^{\frac{1}{2}}$ rather than (time)$^{\frac{1}{3}}$ as in the theory, whereas the data for acetic acid were in close agreement with the theory. The predicted values of the departure time of the bubbles were in good agreement with the data, especially at the larger superheats.

NOMENCLATURE

a, radius of bubble;
A, growth constant, equation (17);
B, growth constant, equation (20);
c, $2s$;
C_G, C_L, specific heat of gas, liquid;
D, diameter of bubble;
f, frequency of bubbling;
k, thermal conductivity;
L, latent heat of vaporization;
r_0, radius of nucleation cavity;
Re, $2aU/\nu$, Reynolds number;
s, distance travelled by centre of bubble;
t, time;
t_0, time at which $a = r_0$;
t_B, fictitious time in equation (20);
T, temperature;
U, velocity of centre of bubble;
We_d, $2a_dU_d^2\rho_L/\sigma$, Weber number at departure conditions;
α, thermal diffusivity;
β, growth constant, equation (10);
ν, kinematic viscosity;
ρ_G, ρ_L, density of gas, liquid;
σ, surface tension;
τ, $t + t_0$.

Subscripts

d, evaluated at end of departure stage;
$*$, evaluated at end of growing stage.

INTRODUCTION

THE PREDICTION of the bubbling frequency and the departure diameter is of central importance in the theoretical study of nucleate boiling. This is because the heat flux from a hot surface is related to the volumetric flowrate of vapour formed, which is proportional to fD^3. A number of authors [1–5] have proposed empirical or semi-empirical equations relating f and D, but as has been pointed out by Ivey [5] there is considerable divergence not only in the correlations but also in the experimental data. Other attempts include those of Fritz [6], which

† Present address: C.O.P.P.E., Federal University of Rio de Janeiro, Brazil.

involved a balance of buoyancy and surface tension forces at breakoff, and Witze *et al.* [7] who neglected surface tension and established the breakoff condition as a balance between liquid inertia and buoyancy. As will be shown, both of these approaches are over-simplifications.

The problem of nucleate pool boiling as treated by these authors is complicated by the non-uniformity of the temperature field, and the transfer of heat from a wall to the liquid. In this work we treat the simpler case of boiling at a nucleation site in a uniformly superheated liquid. Here it is permissible to regard the bubble as growing in an infinite liquid, initially at a uniform temperature. Thus the energy and momentum equations can be solved separately, with appropriate simplifications, to yield the bubble radius and distance from the initial position as functions of time. Obviously there are certain differences between this problem and the pool boiling case. However, simplifications on the heat transfer side enable much greater insight into the fluid mechanics of the problem.

An essential part of the theoretical model is the determination of the radius $a(t)$ of a bubble growing at a point in a uniformly superheated liquid. This problem was first attacked by Bošnjaković [8], and extended and refined by Forster and Zuber [9] and Plesset and Zwick [10]. It was assumed that bubble growth is limited by heat transfer to the phase interface, both conductive and convective terms being important. Scriven [11] has shown that the results of these workers are valid, providing the growth rate and the dimensionless superheat are sufficiently large. Experimental investigations into the validity of these results have been conducted by Dergarabedian [12] and Darby [13]. In both these works the bubbles were observed while in free rise so that it was not possible to remove the convective effects due to the relative motion of the bubbles and the liquid. In fact, Dergarabedian found that the bubble radius depended on $t^{\frac{1}{2}}$ while Darby found better agreement with $t^{\frac{1}{4}}$. Kosky [14] also found the $t^{\frac{1}{4}}$ variation. However, in view of the uncertainty on this point, we have used the theoretical work as a guide. Where the theory has been found to be inadequate we have resorted to curve-fitting of the experimental measurements.

THEORY

Consider a spherical bubble growing at a nucleation site on a horizontal plate in a uniformly superheated liquid. It is assumed that bubble formation takes place in three stages: expansion, transition and waiting. The position of the bubble relative to the nucleation site is shown for each stage in Fig. 1.

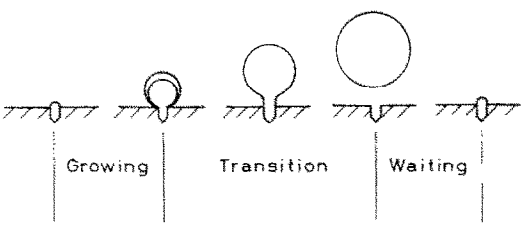

FIG. 1. Idealized stages in bubble formation and departure.

(a) During the growing or *expansion* stage the spherical bubble grows by evaporation of the liquid. The inertial reaction of the liquid and the surface tension force exceed the upward buoyancy force so the bubble remains attached to the cavity. The centre of the bubble moves upward with velocity equal to the rate of increase of the bubble-radius.

(b) *Transition* stage. With increasing time the buoyancy overcomes the downward forces and the bubble rises free from the cavity, although still attached by a short neck. The bubble, while continuing to grow by evaporation, undergoes a sudden acceleration at the onset of this stage. The instant in time when the transition stage commences will be called the *transition time.* The stage ends when the neck breaks and the bubble rises free.

(c) The *waiting* stage comprises the time from when the bubble departs to when the next begins to grow. The duration of this stage is determined by phenomena in or near the nucleation site, such as liquid penetration and evaporation inside the cavity.

In setting up a mathematical description of the process, it is assumed that single bubbles are formed and released one at a time and there is no interaction between successive bubbles. Viscous effects are neglected, a step which will be justified later, and so the liquid is taken to be inviscid, incompressible and irrotational. This enables the velocity fields to be represented by a velocity potential. Since the density of the gas vapour is very small it may be assumed that there are no pressure variations within the bubble. Thermodynamic equilibrium is postulated at the gas–liquid interface.

In terms of the velocity potential ϕ, the equation of continuity is Laplaces equation, $\nabla^2\phi = 0$, which must be solved with the appropriate boundary conditions. Since this equation is linear, we may simply find one solution ϕ_E to represent the flow around an expanding sphere, and another ϕ_T representing the translatory motion of a sphere moving with velocity U normal to a plane wall. In both cases it is essential to take into account the presence of the wall. The potential of the total motion ϕ is then the sum of ϕ_E and ϕ_T. Using the method of images we find

$$\phi = U\left(\frac{a^3}{2r^2} + \frac{a^3 r}{c^3} + \frac{a^6 r}{c^6} + \frac{a^9}{2c^3 r^2} + \frac{a^9}{2c^6 r^2}\right)\cos\theta + \frac{\dot{a}a^2}{r} + \dot{a}\left(\frac{a^2 r}{c^2} + \frac{a^5}{2c^2 r^2} + \frac{a^5 r}{c^5} + \frac{a^8}{2c^5 r^2}\right)\cos\theta \qquad (1)$$

with $c = 2s$, $U = \mathrm{d}s/\mathrm{d}t$, $\dot{a} = \mathrm{d}a/\mathrm{d}t$, and s being the height of the centre of the bubble above the flat plate. The coordinate system is shown in Fig. 2. In (1), terms smaller than a^6/s^6 have been neglected since $a/s < 1$ always.

The pressure distribution in the liquid is given by Bernoulli's equation:

$$\frac{p}{\rho_L} = \frac{\partial\phi}{\partial t} - \tfrac{1}{2}q^2 - g(s + r\cos\theta) + \frac{P_\infty}{\rho_L} \qquad (2)$$

where P_∞ is the liquid pressure at the level of the cavity in the absence of motion and q is the

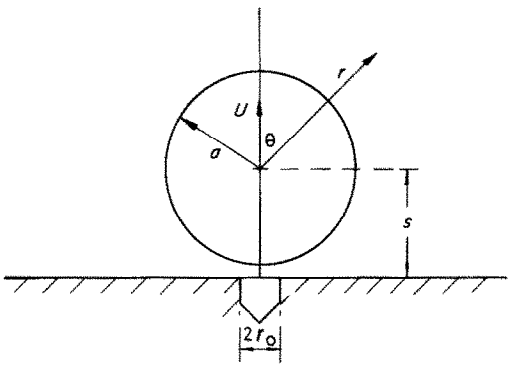

FIG. 2. The coordinate system.

absolute velocity. By integrating the vertical component of the pressure over the surface of the bubble, the force of inertia and buoyancy is obtained:

$$F_I = 2\pi\rho_L\left\{\frac{a^3}{3}\frac{\mathrm{d}^2 s}{\mathrm{d}t^2}\left(1 + \frac{3a^3}{c^3} + \frac{3a^6}{c^6}\right) - \frac{6a^6}{c^4}\left(\frac{\mathrm{d}s}{\mathrm{d}t}\right)^2\left(1 + \frac{2a^3}{c^3}\right) + \frac{a^5}{c^2}\frac{\mathrm{d}^2 a}{\mathrm{d}t^2}\left(1 + \frac{a^3}{c^3}\right) + a^2\frac{\mathrm{d}s}{\mathrm{d}t}\frac{\mathrm{d}a}{\mathrm{d}t}\left(1 - \frac{3a^6}{c^6}\right) + 3\frac{a^4}{c^2}\left(\frac{\mathrm{d}a}{\mathrm{d}t}\right)^2\left(1 + \frac{2a^3}{c^3}\right) - \tfrac{2}{3}ga^3\right\}. \qquad (3)$$

The first part of this expression represents the inertial reaction of the liquid, and opposes the motion of the bubble; the last term arises from the buoyancy of the bubble.

The other force acting on the bubble is that of surface tension at the nucleation site. If the

radius of the nucleation cavity is r_0, the resulting force is

$$F_s = 2\pi r_0. \tag{4}$$

The equation of motion for the bubble may now be written:

$$F_T = F_s + F_I = \frac{4}{3}\pi\rho_G a^3 \frac{dU}{dt}. \tag{5}$$

Since the density ρ_G of the vapour is very small, the right hand side of this equation may be neglected. Thus we find

$$\frac{F_T}{2\pi\rho_L} = \tfrac{1}{3}a^3E_1\frac{d^2s}{dt^2} - 6a^2E_2\left(\frac{ds}{dt}\right)^2 + a^3E_3\frac{d^2a}{dt^2} + \frac{r_0\sigma}{\rho_L} + a^2E_4\frac{ds}{dt}\frac{da}{dt} + 3a^2E_5\left(\frac{da}{dt}\right)^2 - \frac{2ga^3}{3} = 0 \tag{6}$$

where

$$E_1 = 1 + 3\left(\frac{a}{c}\right)^3 + 3\left(\frac{a}{c}\right)^6$$

$$E_2 = \left(\frac{a}{c}\right)^4\left[1 + 2\left(\frac{a}{c}\right)^3\right]$$

$$E_3 = \left(\frac{a}{c}\right)^2\left[1 + \left(\frac{a}{c}\right)^3\right]$$

$$E_4 = 1 - 3\left(\frac{a}{c}\right)^6$$

$$E_5 = \left(\frac{a}{c}\right)^2\left[1 + 2\left(\frac{a}{c}\right)^3\right]$$

or, after rearrangement,

$$\frac{dU}{dt} = 18\frac{U^2E_2}{aE_1} - 3\ddot{a}\frac{E_3}{E_1} - 3\frac{U\dot{a}}{a}\frac{E_4}{E_1} - 9\frac{\dot{a}^2E_5}{aE_1} + \frac{2g}{E_1} - \frac{3r_0\sigma}{a^3\rho_LE_1} \tag{7}$$

with

$$U = \frac{ds}{dt}, \quad \dot{a} = \frac{da}{dt}, \quad \ddot{a} = \frac{d^2a}{dt^2}.$$

During the expansion stage, the bubble is, as it were, pressed down on the flat plate by the reaction of the liquid, although still remaining spherical. Thus $s \equiv a$, $U \equiv \dot{a}$ and $dU/dt \equiv \ddot{a}$, and the equation of motion simplifies to

$$\frac{145}{192}\ddot{a}a^3 + \frac{91}{64}\dot{a}^2a^2 + \frac{r_0}{\rho_L} \geqslant \frac{2ga}{3} \tag{8}$$

where the inequality sign is necessary because the bubble is not free to move beneath the plate. However, with increasing time the dominance of the left-hand side is eroded and the first stage ends when the two sides become precisely equal, and the bubble can lift off the plate. From this time onward the bubble, while still growing, rises with $s > a$, and the velocity U must be found from the general expression [7].

The initial condition for the expansion stage is that at $t = 0$, $a = a_0 = r_0$. Thus bubble growth is considered to commence when the radius is equal to the radius of the nucleation cavity.

Rate of bubble expansion

It is evident from the equations presented above that the bubble dynamics can be followed in the expansion and transition stage if a, $\dot{a}$ and $\ddot{a}$ are known as functions of time. For theoretical predictions we can use the work of Scriven [11]:

$$a = 2\beta(\alpha\tau)^{\frac{1}{2}} \tag{9}$$

$$\beta = \left(\frac{3}{\pi}\right)^{\frac{1}{2}}\Delta T\left[\frac{\rho_G}{\rho_L}\left(\frac{L}{C_L} + \frac{(C_L - C_G)}{C_L}\Delta T\right)\right]^{-1}. \tag{10}$$

These expressions are valid for large values of the "growth constant" β and of the dimensionless superheat $C_L\Delta T/L$. These conditions have been strictly satisfied in the experiments reported here.

Criteria for transition from one stage to the next

During the expansion stage, the distance travelled by the centre of the bubble is equal to the bubble radius. Thus

$$s = a = 2(\alpha\tau)^{\frac{1}{2}} \tag{11}$$

and

$$U = \frac{ds}{dt} = \dot{a} = \beta\left(\frac{\alpha}{\tau}\right)^{\frac{1}{2}}. \quad (12)$$

If there were no buoyancy effect, the rising velocity would become smaller and smaller as the bubble expanded. However, with increasing time the buoyancy does come into play and the rising velocity of the bubble will start to increase. At the time τ_* at which the expansion stage ends and the transition stage begins, the upward and downward forces on the bubble come into equilibrium. It is reasonable to assume that at this critical time τ_* the upward velocity ds/dt has reached a minimum so that the term in d^2s/dt^2 is zero. Thus equation (8) becomes:

$$\frac{91}{64}\dot{a}_*^2 a_*^2 + \frac{r_0\sigma}{\rho_L} = \frac{2}{3}ga_*^3 \quad (13)$$

which yields as a solution:

$$\tau_*^{\frac{1}{2}} = \frac{273\beta\alpha^{\frac{1}{2}}}{256g}\left(1 + \frac{16r_0\sigma}{91\rho_L\beta^4\alpha^2}\right). \quad (14)$$

The magnitude of τ_* is clearly dependent on the physical properties of the boiling system and the cavity size. At a given cavity, increasing the superheating temperature gives a larger β and a smaller τ_*. At low superheating temperatures, the effect of liquid inertia is small compared with the surface tension in (13), and the solution simplifies to

$$\tau_*^{\frac{1}{2}} = \frac{3r_0\sigma}{16\rho_L g\beta^3\alpha^{\frac{1}{2}}}. \quad (15)$$

In heterogeneous boiling most of the heat is transferred from the solid to the liquid during the time the bubble remains in contact with the hot wall. The above expressions for τ_* are useful in providing an estimate of this contact time.

To determine the criterion for detachment of the bubble from the nucleation site resort has been made to experiment. Observations on the various systems used indicate that detachment occurs when

$$\frac{s}{a} \simeq 1{\cdot}54. \quad (16)$$

EXPERIMENTAL

The experimental techniques used in this work have been developed from those of Dergarabedian [12]. A diagrammatic sketch of the apparatus is shown in Fig. 3. The liquid is heated

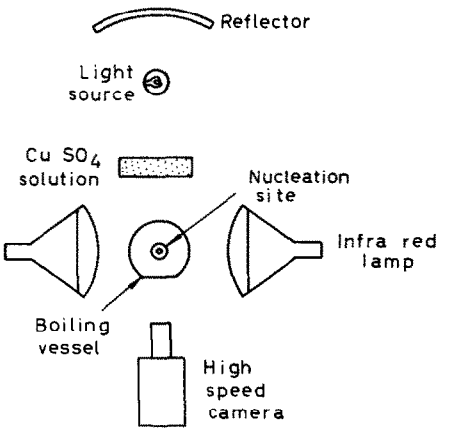

FIG. 3. Diagrammatic sketch of apparatus.

in a glass container by two directly opposed 250 W infra-red lamps, controllable through a Variac transformer. Temperatures were measured by a mercury-in-glass thermometer, calibrated to 0·1°C. The vessel was provided with an optically flat glass window to remove distortion of the image of the bubble.

The nucleation cavity was formed on the end of a glass rod, bent in the form of a U so that while the rod was suspended from above, the cavity opening was vertically upward. The cavity was made by drawing out thick-walled glass capillary tubing. The cavity radius was 220 μ, and its length was 4·6 mm.

The following procedure was carried out before each experiment was conducted. The vessel and the cavity rod were cleaned with chromic acid, washed and dried. The liquid to be used in the experiment was poured into the vessel to a level about 6 cm above the glass window, and heated at the base by an electric heater. The liquid was boiled for about 20 min to eliminate dissolved gases and to provoke

nucleate boiling at nucleation sites on the sides of the vessel, and especially in the vicinity of the window. On cooling the liquid to about 10°C below the boiling point, these cavities filled with liquid and became inactive. During this boiling step, the vapour formed was condensed and returned to the vessel by a glass reflux condenser.

The boiled liquid in its container was then placed between the two infra-red lamps and heated at the rate of about 1°C per min, to ensure a uniform temperature distribution. (This rate was found by trial, placing one thermometer near the wall and another at the centreline.) When the temperature exceeded the boiling point the artificial nucleation site was immersed and the heating adjusted to give the required superheat.

be used for $a(t)$. The upper limit was imposed to avoid coalescence between successive bubbles at or near the point of breakoff.

Photographs of the bubble behaviour were taken with a Fairchild HS 101 16 mm motion picture camera of the rotating prism type, in the range 1000–2500 frames per s, using Kodak Plus-X panchromatic film. Accurate timing was obtained from 100 cps light-marks placed on the film edge by a pulse generator. The camera lens system produced $\times 2$ magnification. After development the films were displayed on a motion picture analyser (Vanguard Instrument Corp.) which had a $\times 10$ magnification. The vertical and lateral cross wires could be located with an accuracy of $\pm 0{\cdot}001$ in. Two dimensions were read: (a) the bubble diameter $D = 2a$, which

Table 1. Properties of water and water vapour

T (°C)	$v_L(15)$ (cm³/g)	$v_g(15)$ (cm³/g)	$L(15)$ (cal/g)	$k \times 10^3(16)$ (cal/cm² °C)	$C_L(17)$ (cal/g °C)	$\sigma(18)$ (dyne/cm)	$\alpha \times 10^3$ (cm²/s)
100	1·0435	1673·0	539·1	1·598	1·0076	58·85	1·655
102	1·0450	1565·6	537·9	1·599	1·0082	58·47	1·657
103	1·0458	1515·0	537·2	1·600	1·0085	58·29	1·659
104	1·0466	1466·3	536·6	1·601	1·0088	58·10	1·661

Table 2. Properties of acetic acid

T (°C)	$\rho_L(19)$ (g/cm³)	$\rho_G(19) \times 10^3$ (g/cm³)	$L(18)$ (g/cm³)	$k \times 10^4(20)$ (cal/cm² °C)	$C_L(18)$ (cal/g °C)	$\sigma(18)$ (dyne/cm)	$\alpha \times 10^3$ (cm²/s)
118	0·9368	3·15	96·89	3·627	0·5787	18·10	0·6677
120	0·9386	3·30	96·67	3·617	0·5806	17·91	0·6654
121	0·9348	3·41	96·56	3·612	0·5815	17·81	0·6645
122	0·9335	3·52	96·45	3·607	0·5824	17·71	0·6635
123	0·9321	3·63	96·35	3·602	0·5834	17·62	0·6624
124	0·9308	3·74	96·24	3·598	0·5843	17·52	0·6616

Two liquids were used, acetic acid (A.R. grade), B.P. 118·0°C, and distilled water (B.P. 100·0°C). The levels of superheat at which experiments were conducted were (a) acetic acid: 2·0, 3·0, 4·0, 5·0 and 6·0°C and (b) water: 2·0, 3·0 and 4·0°C. The lower limit was mainly determined by the desire to maintain large values of the growth constant β, equation (10), to enable the approximate asymptotic theory to

was the maximum horizontal dimension of the bubble, and (b) the distance s travelled by the centre of the bubble. These distances are shown in Fig. 2. During the time when the bubbles were attached to the cavity it was observed that they were very close to spherical in shape except for the small tail which existed in the transition stage. However, after breakoff they tended to be spheroidal, and the dimension D would not

be appropriate. The behaviour after breakoff does not concern us here.

The physical data needed in the calculations are shown in Tables 1 and 2 together with the source references. In some cases, interpolation of published figures was necessary. The thermal diffusivity $\alpha = k_L/\rho_L C_L$ was calculated from its constituents.

RESULTS AND DISCUSSION

Bubble growth rates

Measured values of the bubble radius as a function of time for acetic acid are given in Fig. 4. The points are recorded from the initial bubble size $a = r_0$ until the instant of breakoff. There is an uncertainty of up to $1{\cdot}4 \times 10^{-3}$ s in the determination of the time at which growth starts, this being the time between successive frames on the film. The bubble radii are expressed in dimensionless form (a/r_0) for representational convenience.

All the data are well represented by expressions of the form

$$a = A\tau^{\frac{1}{2}} = A(t + t_0)^{\frac{1}{2}}. \tag{17}$$

The broken lines on Fig. 4 represent this

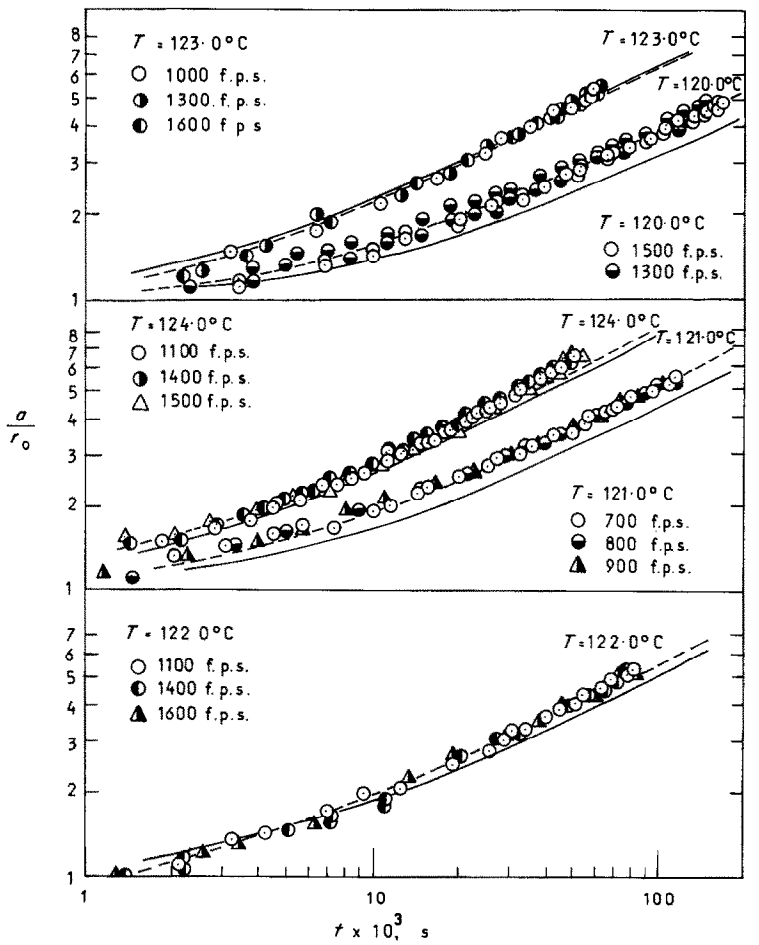

FIG. 4. Bubble radius for acetic acid (B.Pt. 118·0°C). The experimental time is measured from the cine frame on which $a = r_0$ was first observed.

equation, with the constants A, t_0, being found by the method of least squares. Comparisons of (9) with (17) shows that A is related to the theoretical growth constant β by

$$A = 2\beta\alpha^{\frac{1}{2}} \tag{18}$$

provided the time scale is displaced by t_0, this being interpreted as the time taken for the bubble to grow from zero radius to $a = r_0$, that is

$$t_0 = (r_0/2\beta\alpha^{\frac{1}{2}})^2. \tag{19}$$

Table 3 contains values of the experimental parameters A, t_0 obtained by curve fitting, and $a_0 = r_0 = 0{\cdot}022$ cm. The data points refer to bubble growth up to the point of departure. The error in determining the zero time, at which $a = r_0$, is about $5\text{–}7 \times 10^{-4}$ s.

When the data were fitted to the square-root-of-time law [17] values of A and t_0 could be found by the method of least squares. Excellent agreement was found between the experimental values of A and the prediction from $A = 2\beta\alpha^{\frac{1}{2}}$ as shown in Table 4. However, the values of t_0 were all negative, indicating that the assumed time dependence was incorrect at small times. The continuous curves in Fig. 5 represent

Table 3. Experimental and theoretical growth parameters for acetic acid (B. Pt. 118°C)

	Experimental equation (17)		Theoretical		
T (°C)	A (cm/s$^{\frac{1}{2}}$)	t_0 (s)	β (Scriven [11])	$A = 2\beta\alpha^{\frac{1}{2}}$ (cm/s$^{\frac{1}{2}}$)	t_0 (s)
120	0·258	0·0079	3·447	0·178	0·0153
121	0·363	0·0040	5·146	0·265	0·0069
122	0·384	0·0024	6·830	0·352	0·0039
123	0·426	0·0024	8·499	0·438	0·0025
124	0·532	0·0022	10·149	0·522	0·0018

also the predicted values from (18) and (19), with $r_0 = 0{\cdot}022$ cm. It is seen that for the largest superheats the agreement is very good indeed, while at the smallest ΔT, the predicted growth constant is too small. This is also shown in the solid lines in Fig. 4, where a is calculated by the approximate theory, equations (17)–(19). For the smallest ΔT the predicted radii are about 20 per cent too low, whereas for $\Delta T = 4$, 5 and 6°C, the agreement is very good.

It can be seen that for the largest superheat near the instant of release from the cavity, the data points deviate slightly from the $\tau^{\frac{1}{2}}$ curve with a slightly increased slope. This is possibly a result of the translatory motion (Tokuda *et al.* [23]).

The results for boiling water are given in Fig. 5, for superheats of 2, 3 and 4°C. The initial bubble radius is the same as that for acetic acid, $a = A(t + t_0)^{\frac{1}{2}}$ with the experimentally determined A and t_0. For computational purposes it was found that the data could be much better represented by

$$a = B(t + t_B)^{\frac{1}{2}} \tag{20}$$

where B, t_B were found by curve fitting, and are given in Table 4. Equation (20) with appropriate constraints is shown in Fig. 5 by the broken lines. The time exponent greater than $\frac{1}{2}$ has also been reported in earlier experiments [13, 22].

Translational motion of the centre of the bubble

Knowing the rate of bubble growth with time, it is possible to solve the equations of motion to find $s(t)$ and the criteria for termination of the expansion stage, and the moment of detachment of the bubble. During the expansion stage the solutions for $a \equiv s$ may be found from (17) and

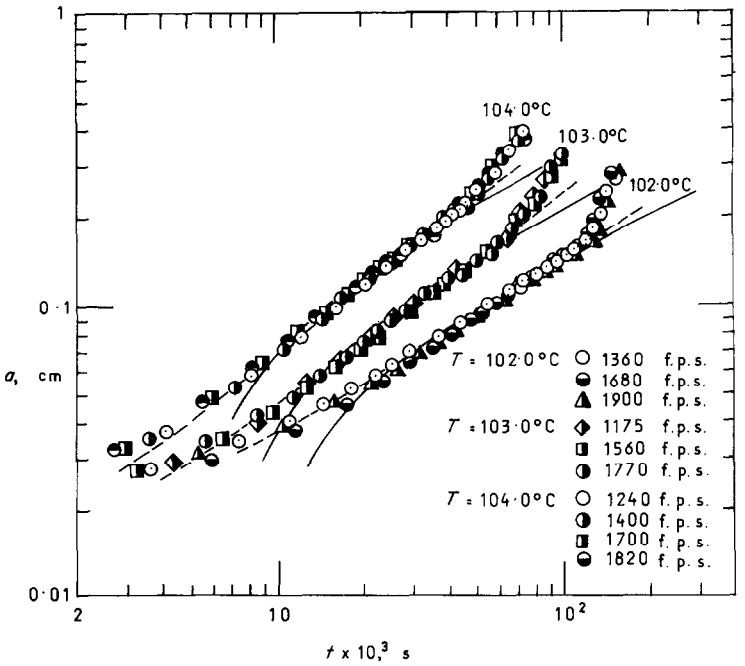

FIG. 5. Radius of steam bubble at three superheats.

Table 4. Experimental and theoretical growth parameters for water (B. Pt. 100°C)

	Theoretical			Experimental equation (17)		Experimental equation (20)	
T (°C)	β [11]	A (cm/s$^{\frac{1}{2}}$)	t_0 (s)	A (cm/s$^{\frac{1}{2}}$)	t_0 (s)	B (cm/s$^{\frac{1}{2}}$)	t_B (s)
102	5·843	0·476	0·0021	0·470	−0·0088	0·756	0·0075
103	8·754	0·713	0·0014	0·694	−0·0073	1·348	0·0013
104	11·658	0·950	0·0005	1·035	−0·0054	2·190	0·0001

(20) and the transition time τ_* may also be found analytically.

Once the bubble has started to rise free of the surface the motion of the centre of the bubble is found from (7) with values of a, $\dot{a}$ and $\ddot{a}$ obtained from (17) or (20), whichever is appropriate. The integration of the equation of motion was carried out numerically using a fourth order Runge–Kutta procedure, with a time interval of 0·003 s. This is a straightforward calculation which gives s and U until the breakoff criterion is satisfied and the bubble detaches. During free rise the trajectory can be calculated for a short distance by omitting the surface tension term in the equation of motion (7).

It should be noted that a geometrical correction was introduced to account for the fact that the bubble is not actually a sphere, but is a segment of a sphere. The bubble is a hemisphere at zero time and it grows like a spherical sector. Hence the theoretical curves were calculated from

$$s = a[1 - (r_0/a)^2]^{\frac{1}{2}}$$

and

$$\frac{U}{\dot{a}} = [1 - (r_0/a)^2]^{-\frac{1}{2}}.$$

Experimental measurements of the height s of the bubble centre are given in Figs. 6–8 together with the predictions. The agreement at the lowest superheats is good, but at the largest ΔT, some divergence is noted as the bubble nears detachment.

$$t_* = \tau_* - t_0$$

was used where the appropriate experimental value for t_0 (or t_B) was used in each case. Although it is a highly subjective matter to decide when each of the curves for $s(t)$ displays the change in slope expected at the transition time, the predictions appear to be entirely reasonable.

The theoretical curves in Figs. 6–8 terminate at the point of departure. The locus of the

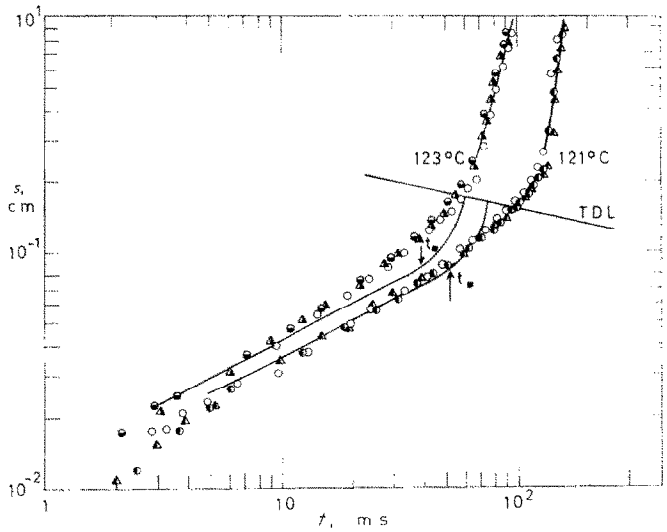

FIG. 6. Acetic acid: measurements of the distance travelled by the centre of the bubble for acetic acid boiling at superheats of 3·0 and 5·0°C. The "theoretical departure line" (TDL) is the locus of the distances at which bubble departure is predicted.

$T = 121$°C	$T = 123$°C
○ 620 f.p.s.	○ 1060 f.p.s.
◐ 817 f.p.s.	◒ 1400 f.p.s.
▲ 1020 f.p.s.	▲ 1650 f.p.s.

The time at which the expansion stage ends, τ_*, was calculated from (14) with experimentally determined values of A to calculate $\beta = A/2\alpha^{\frac{1}{2}}$. The time τ_* is of course relative to the time t_0 when the bubble starts to grow, so that in entering the predicted transition time on Figs. 6–8, the real time

terminal points has been drawn as the "Theoretical Departure Line" (TDL). The theoretical and experimental departure times are compared in Table 5, each experimental result being the mean of four separate determinations. The agreement is very good except for the lowest superheats. Also shown in Table 5 are the

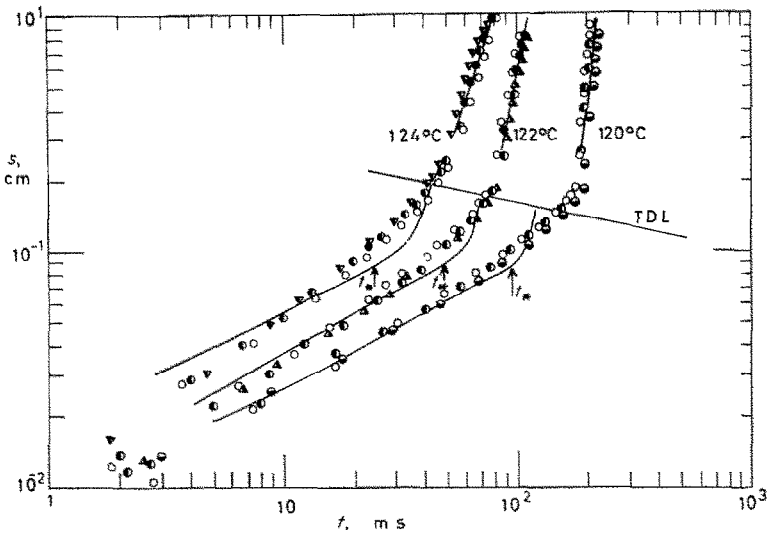

FIG. 7. Acetic acid: measurements of the distance travelled by the centre of the bubble at superheats of 2·0, 4·0 and 6·0°C.

$T = 120°C$	$T = 122°C$	$T = 124°C$
○ 1100 f.p.s.	○ 1100 f.p.s.	○ 1100 f.p.s.
◐ 1500 f.p.s.	◐ 1400 f.p.s.	◐ 1500 f.p.s.
◒ 1700 f.p.s.	▲ 1600 f.p.s.	▼ 1700 f.p.s.

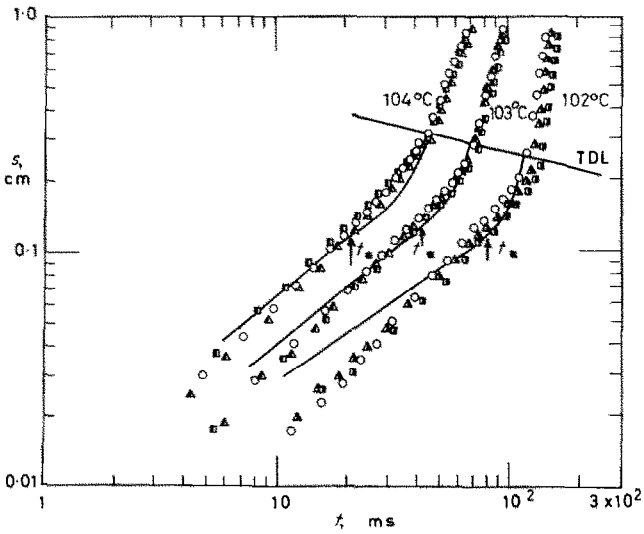

FIG. 8. Water: measurements of the distance travelled by the centre of the bubble for superheats of 2·0, 3·0 and 4·0°C.

$T = 102°C$	$T = 103°C$	$T = 104°C$
○ 1300 f.p.s.	○ 1260 f.p.s.	○ 1250 f.p.s.
▲ 1630 f.p.s.	▲ 1700 f.p.s.	▲ 1625 f.p.s.
◨ 1900 f.p.s.	◧ 1850 f.p.s.	◧ 1820 f.p.s.

observed bubble periods, that is, the inverse of the frequency of bubble formation. In almost all cases the two times are identical, indicating that the next bubble begins to grow immediately after the previous one has broken off. Thus in this type of boiling the "waiting time" is only a very small proportion of the bubbling period.

liquid was heated by a hot surface, and the liquid was by no means uniform in temperature.

Omission of viscous terms

In the theoretical development, viscous effects were entirely neglected. For the bubble growth problem, this step can be justified [11] since the growth is determined by the rate at which heat can be supplied to the gas–liquid interface. Thus viscosity plays no part in determining $a(t)$.

As far as the translational motion $s(t)$ is concerned, viscosity will be unimportant provided the translational Reynolds number is sufficiently high, that is

$$Re = 2aU/v \gg 1$$

during the translational stage. After the bubble has started to rise from the nucleation site, equation (7) shows that dU/dt is of order $2g$ so that

$$U = \frac{ds}{dt} \simeq 2gt.$$

Putting $t \sim 30 \times 10^{-3}$ s, and taking $a \simeq 0{\cdot}2$ cm, the translational Reynolds number for the boiling water is about 1000 (minimum). For acetic acid we may use the velocities in Fig. 10. These correspond to translational Reynolds

Table 5. Bubble properties at breakoff

System	T (°C)	a_d (cm)	s_d (cm)	U_d (cm/s)	We_d	Departure time t_d(s)		Bubble period $1/f$(s^{-1})
						Theoretical	Experimental	
Acetic acid	120·0	0·0965	0·1483	6·80	0·47	0·120	0·180	0·196
	121·0	0·1041	0·1559	8·24	0·72	0·074	0·127	0·127
	122·0	0·1026	0·1581	8·59	0·80	0·069	0·082	0·082
	123·0	0·1050	0·1597	9·02	0·90	0·058	0·062	0·069
	124·0	0·1126	0·1729	10·37	1·29	0·042	0·050	0·055
Water	102·0	0·1489	0·2293	9·86	0·47	0·109	0·124	0·124
	103·0	0·1654	0·2530	12·67	0·87	0·064	0·067	0·067
	104·0	0·1980	0·3034	16·13	1·69	0·042	0·046	0·046

Departure diameter and frequency

Many workers have tried to set up simple correlations to relate the bubbling frequency f with the bubble diameter at departure D. These works have been summarised by Ivey [5]. For a given liquid, the correlations were generally of the form

$$f = AD^n$$

where A is a constant, sometimes dependent on the physical properties, and the exponent n has been given values between $-\frac{1}{2}$ and -3. Figure 9 shows experimental points from Ivey [5] together with the experimental values of f and D from the present work. It is apparent that there is a completely different dependence of f on D, the exponent n having a positive value of approximately $n = 2$. This is undoubtedly due to the difference in the heat transfer mechanism. In our case the liquid is uniformly superheated and heat is conducted uniformly from the surroundings. In all the data quoted by Ivey, the

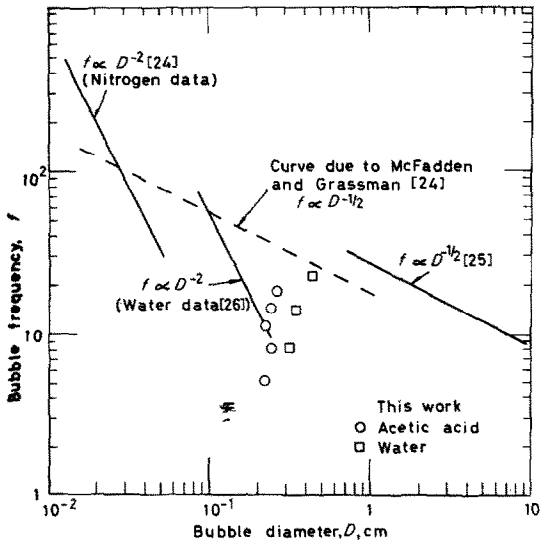

FIG. 9. Comparison of measured bubbling frequency (s^{-1}) with data from the literature.

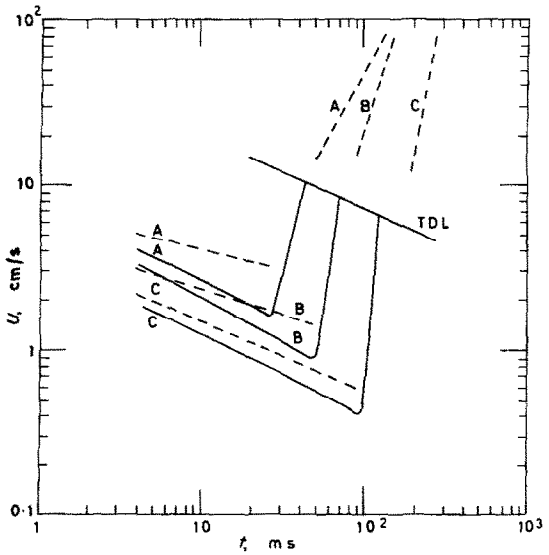

FIG. 10. Rising velocity of the centre of the bubble as a function of time. The continuous lines are from the theory while the dashed curves are from smoothed experimental data. Acetic acid at temperatures of 124·0°C (A), 122·0°C (B), 120·0°C (C).

numbers in the range 100–1000. Since these Reynolds numbers are very large, it is concluded that the viscous stresses are negligible in comparison with the inertial pressures, and may therefore be neglected.

Bubble velocity at departure

It is tempting to assume, in setting up a simplified model for growth and departure of single bubbles, that the rising velocity at departure is equal to the instantaneous rate of radial expansion $\dot{a}$. This assumption was in fact made by Hamburger [21], but it appears that it could be in error by an order of magnitude. Figure 10 shows the rising velocity U as a function of time for acetic acid. The continuous line is from the present theory, while the dashed lines are taken from the smoothed experimental data. Up to the end of the expansion stage U decreases. However the results indicate that while the bubbles are rising and still attached to the cavity, the velocity of the centre of the bubble increases very much over a short time interval so that at departure the bubble is rising rapidly.

The Weber number at departure, $We_d = 2a_d\rho_L U_d^2/\sigma$, has been calculated and is shown in Table 5. The surface tension pressure $(2\sigma/a_d)$ is generally larger, or of the same order, as the inertial pressure $(\frac{1}{2}\rho_L U_d^2)$, explaining why the bubbles tended to remain spherical while attached to the cavity.

CONCLUSIONS

1. A simple model is proposed for the behaviour of a vapour bubble growing at a nucleation site in a uniformly superheated liquid. Two stages of growth are assumed. In the growing stage the spherical bubble rests at the nucleation cavity, and its rising velocity is equal to the rate of increase of the bubble radius. In the translation stage, buoyancy causes the bubble to rise off the wall, and the stage terminates when the bubble breaks free.

Using a theory based on this model the radius and departure time of the vapour bubbles has been predicted. The results are in good agreement with the experiments especially at the larger superheats.

2. The theoretically predicted bubble growth rates giving the radius proportional to $(\text{time})^{\frac{1}{2}}$ are in good agreement with the experiments

for acetic acid. However, for boiling water, the radius appears to vary as (time)$^{\frac{1}{4}}$.

3. For the type of boiling considered here, the "waiting time" between the departure of one bubble and the inception of the next at a particular nucleation site, is effectively zero except at the lowest superheats. Thus the bubbling frequency is the inverse of the "departure time".

4. The bubble velocity at departure was found to be an order of magnitude higher than the rate of radial expansion. This is because the bubble expands like $da/dt \propto \tau^{-\frac{1}{2}}$ (or $\tau^{\frac{1}{4}}$ for steam), whereas the translational velocity at departure is determined by the rise of the bubble during the transition stage under the action of buoyancy.

ACKNOWLEDGEMENT

One of us (M.S.) is grateful to the Conselho Nacional de Pesquisas, Brazil and to the British Council for financial support.

REFERENCES

1. R. Cole, A photographic study of pool boiling in the region of critical heat flux. *A.I.Ch.E.Jl* **6**, 533 (1960).
2. P. W. McFadden and P. Grassman, The relation between bubble frequency and diameter in nucleate pool boiling. *Int. J. Heat Mass Transfer* **5**, 169 (1962).
3. N. Zuber, Hydrodynamic aspects of boiling heat transfer. A.E.C.U. Report No. 4439, (1959).
4. R. Cole, Bubble frequencies and departure volumes at subatmospheric pressures. *A.I.Ch.E.Jl* **13**, 779 (1967).
5. H. J. Ivey, Relationships between bubble frequency, departure diameter and rise velocity in nucleate boiling. *Int. J. Heat Mass Transfer* **10**, 1023 (1967).
6. W. Fritz, Berechnung des maximal Volumen von Dampfblasen. *Phys. Z.* **36**, 379 (1935).
7. C. P. Witze, V. E. Schrock and P. L. Chambre, Flow about a growing sphere in contact with a plane surface. *Int. J. Heat Mass Transfer* **11**, 1637 (1968).
8. F. Bošnjaković, Verdampfung und Flüssigkeitsüberhitzung. *Tech. Mech. Thermo-Dynam. Berl.* **1**, 358 (1930).
9. H. K. Forster and N. Zuber, Growth of a vapour bubble in superheated liquid. *J. Appl. Phys.* **25**, 474 (1954).
10. M. S. Plesset and S. A. Zwick, The growth of vapour bubbles in superheated liquids. *J. Appl. Phys.* **25**, 493 (1954).
11. L. E. Scriven, On the dynamics of phase growth. *Chem. Engng Sci.* **10**, 1 (1959).
12. P. Dergarabedian, The rate of growth of vapour bubbles in superheated water. *J. Appl. Mech.* **20**, 537 (1953).
13. R. Darby, The dynamics of vapour bubbles in nucleate boiling. *Chem. Engng. Sci.* **19**, 39 (1964).
14. P. G. Kosky, Bubble growth measurements in uniformly superheated liquids. *Chem. Engng Sci.* **23**, 695 (1968).
15. R. W. Bain, *Steam Tables.* National Engineering Laboratory, H.M.S.O. Edinburgh (1964).
15. R. W. Bain, *Steam Tables.* National Engineering Laboratory, H.M.S.O. Edinburgh, (1964).
16. *Handbook of Chemistry and Physics*, 46th Edn. Chemical Rubber Co., Cleveland, Ohio. (1964).
17. R. H. Perry, *Handbook of Chemical Engineering*, 4th Edn. McGraw-Hill, New York (1963).
18. *International Critical Tables.* McGraw-Hill, New York (1926).
19. J. Timmermans, *Physical Chemical Constants of Organic Compounds.* Elsevier, New York (1965).
20. N. V. Tsederberg, *Thermal Conductivity of Gases and Liquids.* Arnold, London (1965).
21. L. G. Hamburger, On the growth and rise of individual bubbles in nucleate pool boiling. *Int. J. Heat Mass Transfer* **8**, 1369 (1965).
22. M. Akiyama, F. Tachibana and H. Kawashima, Bubble growth rate in transient boiling, *J. Nucl. Sci. Technol.* **5**, 43 (1968).
23. N. Tokuda, W. J. Yang and J. A. Clark, Dynamics of moving gas bubbles in injection gas cooling. *J. Heat Transfer* **13C**, 371–378 (1968).
24. P. W. McFadden and P. Grassman, The relation between bubble frequency and diameter during nucleate boiling. *Int. J. Heat Mass Transfer* **5**, 169 (1962).
25. R. Cole, A photographic study of pool boiling in the region of the critical heat flux. *A.I.Ch.E.Jl* **6**, 533 (1960).
26. A. P. Hatton and I. S. Hall, Photographic study of boiling on prepared surfaces. Paper No. 115, Third International Heat Transfer Congress, Chicage (1966).

DETERMINATION DU DIAMETRE DE SEPARATION ET DE LA FREQUENCE DES BULLES DANS L'EBULLITION NUCLEEE DES LIQUIDES UNIFORMEMENT SURCHAUFFES

Résumé—On présente une théorie pour décrire le mouvement des bulles de vapeur se développant à un site de nucléation dans un liquide uniformément surchauffé. En incluant la théorie classique de la phase de croissance sphérique les équations du mouvement de translation sont résolues permettant le calcul, en fonction du temps, du rayon et de la position de la bulle.

Les résultats théoriques sont comparés avec l'expérience à partir de l'eau et de l'acide acétique. Pour l'eau le rayon de bulle varie suivant la puissance $\frac{3}{4}$ du temps plutôt que $\frac{1}{2}$ comme dans la théorie, tandis que pour l'acide acétique il y a accord étroit avec la théorie. Les valeurs calculées du temps de décrochage des bulles sont en bon accord avec l'expérience, spécialement aux plus grandes surchauffes.

BESTIMMUNG DES ABREISSDURCHMESSERS UND DER BLASENFREQUENZ BEIM BLASENSIEDEN IN GLEICHMÄSSIG ÜBERHITZTEN FLÜSSIGKEITEN.

Zusammenfassung—Es wird eine Theorie vorgelegt zur Beschreibung der Bewegung von Dampfblasen, die an einer Keimstelle in einer überhitzten Flüssigkeit wachsen. Unter Einbeziehung der klassischen Theorie für sphärisches Blasenwachstum wurden die *translatorischen* Bewegungsgleichungen gelöst, woraus sich Radius und Stellung der Blase als eine Funktion der Zeit bestimmen lassen. Die theoretischen Ergebnisse werden mit Experimenten verglichen, an den Flüssigkeiten Wasser und Essigsäure. Für Wasser zeigte sich der Blasenradius veränderlich mit der (Zeit)$^{\frac{1}{2}}$, mehr als mit der (Zeit)$^{\frac{1}{4}}$, wie die Theorie verlangt, während die Werte für Essigsäure sehr genau mit der Theorie übereinstimmten. Die berechneten Werte für die Blasenablösezeit waren in guter Übereinstimmung mit den Versuchswerten, besonders bei grösserer Überhitzung.

РАСЧЕТ ДИАМЕТРА ОТРЫВА И ЧАСТОТЫ ПУЗЫРЬКОВ ПРИ ПУЗЫРЬКОВОМ КИПЕНИИ В ОДНОРОДНО ПЕРЕГРЕТЫХ ЖИДКОСТЯХ

Аннотация—Представлена теория описания движения пузырьков пара, растущих на месте зарождения пузырьков в однородно перегретой жидкости. С помощью классической теории роста сферической фазы решены уравнения переходного движения, позволяющие рассчитать радиус и положение пузырька как функцию времени.

Теоретические результаты сравниваются с экспериментами на примере кипящей воды и уксусной кислоты. Найдено, что для воды радиус пузырька меняется как (время)$^{3/4}$ а не (время)$^{1/2}$, как дается в теории, в то время как данные для уксусной кислоты находятся в полном соответствии с теорией. Расчетные значения времени отрыва пузырьков находятся в хорошем согласии с данными, в особенности при больших перегревах.